J. Fluid Mech. (1987), *vol.* 180, *pp.* 171–191
Printed in Great Britain

Vortex excitation of rectangular cylinders with a long side normal to the flow

By YASUHARU NAKAMURA AND TOHRU MATSUKAWA
Research Institute for Applied Mechanics, Kyushu University, Kasuga 816, Japan

(Received 31 January 1986 and in revised form 28 November 1986)

The vortex excitation of rectangular cylinders having side ratios of 0.2, 0.4 and 0.6, with a long side normal to the flow, in a mode of lateral translation, is investigated experimentally in a wind tunnel using free- and forced-oscillation methods. The range of reduced wind speeds investigated, 3–12, includes the vortex-resonance regime. The forced-oscillation experiment includes measurements of the fluctuating lift force at amplitudes up to 10% of the length of a long side. The experiments were also performed on cylinders with a long fixed splitter plate. The results of the measurements show that vortex excitation of a rectangular cylinder is strongly dependent on the side ratio. It is suggested that the critical change of the mean base pressure of an oscillating rectangular cylinder with increasing side ratio is closely correlated with the vortex-excitation characteristics. The concept of vortex excitation as aeroelastic flutter occurring in a fluid–body coupled system is proposed on the basis of the experimental results. The most essential feature of vortex excitation as a coupled flutter is that the fluid subsystem can be set into resonance by the body motion. A rapid phase-angle change in the lift force through vortex resonance produces a large out-of-phase force component which excites the motion of the body subsystem.

1. Introduction

Vortex excitation of a bluff body has received considerable attention from both practical and academic points of view. It can occur in a narrow range of wind speed centred on that at which the frequency of vortex shedding coincides with that of the body displacement (hereinafter referred to as the vortex-resonant speed). Many engineering structures such as tall stacks and long bridges are susceptible to vortex excitation. It often causes fatigue in structural members and sometimes leads to the failure of a complete structure. It is an important and very complicated fluid–solid interaction phenomenon, and many basic questions relating to the interplay between the body movement and the formation and shedding of vortices remain unsolved. A number of papers have been written on this subject, and recent reviews may be found in Sarpkaya (1979) and Bearman (1984).

Rectangular cylinders have been good test bodies for investigating separated-flow flutter. In addition to their simple geometry, they are susceptible to a variety of separated-flow flutter including galloping, torsional flutter and vortex excitation both in bending and in torsion. While much work has been done on vortex excitation of a rectangular cylinder, comparatively few measurements have been presented of the fluctuating pressures and forces experienced by an oscillating rectangular cylinder. These include Wilkinson (1974), Otsuki *et al.* (1974), Nakamura & Mizota (1975), Washizu *et al.* (1978), Nakamura (1979) and Bearman & Obasaju (1982).

Otsuki *et al.* (1974), Nakamura & Mizota (1975) and Washizu *et al.* (1978) measured the fluctuating lift force on oscillating rectangular cylinders with $d/h = 1.0$, 2.0 and 4.0, where d and h are the section dimensions respectively parallel and normal to the flow, in addition to the free-oscillation experiment, to investigate vortex excitation and galloping. It was shown that while vortex excitation of a rectangular cylinder was strongly dependent on the side ratio over the range they examined, the phase angle of the lift force relative to the body motion always underwent a rapid change in passing the vortex-resonance regime.

Wilkinson (1974) and Bearman & Obasaju (1982) measured the fluctuating pressures of an oscillating square cylinder. Bearman & Obasaju noted substantial differences in vortex excitation between a circular cylinder and a square cylinder. The square cylinder showed a much smaller amplification of the fluctuating lift force in the lock-in range, and vortex excitation was limited to a narrow range at the upper end of lock-in.

The present paper is concerned with vortex excitation of rectangular cylinders with $d/h = 0.2$, 0.4 and 0.6. The results of measurement of the mean base pressure, the fluctuating lift force and the velocity fluctuation in the near wake on forced-oscillating rectangular cylinders are presented along with those of the rate of growth of oscillation on freely oscillating rectangular cylinders. Attention is focused on the important role of the afterbody shape in vortex excitation of a bluff body. The mechanism of onset of vortex excitation is discussed in detail on the basis of the experimental results and the concept of vortex excitation as coupled flutter is proposed. Some remarks on the concept of lock-in are also included.

2. Experimental arrangements and procedures

2.1. *Wind tunnel and models*

The experiments were performed in a low-speed wind tunnel with a rectangular working section 3 m high, 0.7 m wide and 2 m long. The section dimensions of the three rectangular-cylinder models used were $h = 15$ cm and $d = 3$, 6 and 9 cm. As is shown in figure 1, the model had circular end plates 45 cm ($= 3h$) in diameter with a separation of 65 cm ($= 4.3h$), and it was mounted horizontally in the working section to allow either free- or forced-oscillation experiments. It was constructed with light plastic plates and a metal backbone tube. Its weight was small, about 0.45 kg, particularly important for the forced-oscillation experiment.

2.2. *Free-oscillation experiment*

In the free-oscillation experiment the model was supported by flexural and coil springs to move in a direction normal to the flow. The displacement of the model was sensed by strain gauges cemented on the flexural springs, and a hot-wire anemometer was used to detect regular vortex shedding behind the model when held stationary. Measurements of the frequency and the logarithmic rate of growth or decay of oscillation at an amplitude of $0.1h$ were made on models in still air and in wind from the displacement signals displayed on a pen-recorder. No measurements were attempted of the steady-state amplitude, which could have been much larger than $0.1h$, because attention here was focused on the small-amplitude behaviour of vortex excitation. The frequency of oscillation in still air and the system damping (logarithmic decrement, corrected for the still-air aerodynamic damping as will be described below) were respectively equal to about $f_y = 5.6$ Hz and $\delta_s = 0.0015$. The value of the mass ratio $\mu = m/\rho h^2$, where m is the gross mass of the model per unit

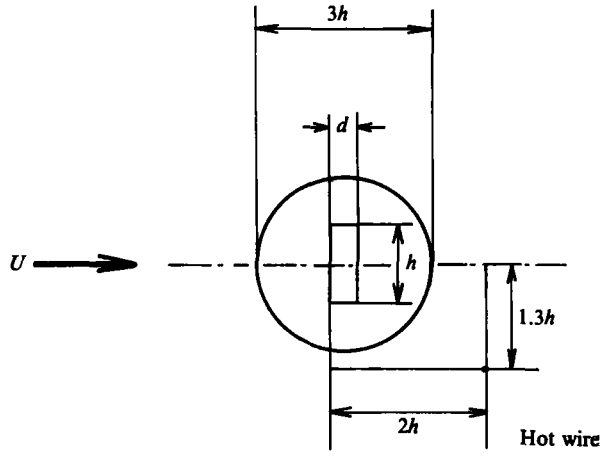

FIGURE 1. Rectangular-cylinder model and hot wire.

span and ρ is the air density, was about 70. The value of the Scruton number which is defined by $Sc = 2\mu\delta_s$ was about 0.2. The wind speed was varied over a range of about 3–10 m s^{-1}. Correspondingly, the reduced wind speed, defined by $\overline{U} = U/(f_y h)$, where U is the wind speed, ranged approximately from 3.5 to 12.0, which included the vortex-resonant speed $\overline{U}_{cr}$. The range of the Reynolds number, which is based on h, was about $(3–10) \times 10^4$. An experiment was added using models with a long splitter plate placed downstream and fixed relative to the tunnel walls. The splitter plate was $6.2h$ in length and the gap between the model and the plate was about $0.03h$.

2.3. *Forced-oscillation experiment*

In the forced-oscillation experiment the model was subjected to simple harmonic lateral oscillation at a constant frequency of 6.0 Hz with an amplitude of 0.05 or $0.1h$ using a mechanical vibrator (Nakamura & Mizota 1975). Measurements of the mean base pressure, the fluctuating lift force and the u-component velocity fluctuation in the wake at a position $2h$ downstream of the leading edge of the model and $1.3h$ off the centreline were made. The range of the wind speed was the same as that for the free-oscillation experiment.

The method for measuring the lift force is as follows. Two identical models, one in a uniform stream and one in still air, are oscillated simultaneously, and the side forces $F(t)$ and $F_1(t)$ acting respectively on the active and the dummy models are measured using strain gauges cemented on the backbone tubes of the models. The lift force on the active model is then obtained by subtracting $F_1(t)$ from $F(t)$. This method conveniently removes the force due to the inertia of the model but, as Bearman & Obasaju (1982) commented, $F_1(t)$ also includes a contribution due to the aerodynamic force acting on the dummy model oscillating in still air.

The aerodynamic force per unit span on a rectangular cylinder oscillating in still air with $y(t) = y_0 \sin 2\pi f_y t$, where y_0 is the amplitude of oscillation, is expressed by

$$F_2(t) = \pi^3 \rho d^2 f_y^2 y_0 (\kappa \sin 2\pi f_y t - \kappa' \cos 2\pi f_y t). \tag{1}$$

The inertia and damping coefficients κ and κ' are functions of two non-dimensional parameters $f_y d^2/\nu$ and y_0/h, where ν is the kinematic viscosity of air. The aerodynamic

d/h	$f_y d^2/\nu$	κ	κ'
0.2	356	3.15	1.00
0.4	1425	2.20	0.28
0.6	3208	2.00	0.17

TABLE 1

force $F_2(t)$ in still air is too small to measure but in still water it is very much larger because of the large water density and can be measured with good accuracy. Therefore, we performed a free-oscillation experiment in still water to determine the values of κ and κ' corresponding to the wind-tunnel experiment. These are shown in table 1. All the results for the lift force presented here have been corrected for the aerodynamic force $F_2(t)$ using the values of κ and κ' shown in table 1.

2.4. *The frequency-response component of the lift force on forced-oscillating cylinders*

Generally, the lift force acting on an oscillating bluff body has two main frequency components: one, which has a frequency equal to that of the imposed oscillation f_y, is hereinafter referred to as the frequency-response component; and the other, which has a frequency equal to that of natural vortex shedding f_v (natural vortex-shedding frequency refers to the frequency that would be measured behind a fixed body under similar flow conditions), is referred to as the Strouhal component.

The frequency-response component of the lift force per unit span is defined in a non-dimensional form as

$$\frac{L_m(t)}{\frac{1}{2}\rho U^2 d} = C_{Lm}(t)$$

$$= C_{Lmo} \sin(2\pi f_y t + \phi_{Lm}), \tag{2}$$

where C_{Lmo} is the amplitude and ϕ_{Lm} is the phase angle relative to the body displacement. A real-time FFT analyser was used to obtain the frequency-response component of the lift force and that of the u-component velocity fluctuation similarly defined.

The condition for the onset of flutter instability is that the out-of-phase component of the lift force is positive, that is,

$$0 < \phi_{Lm} < 180°. \tag{3}$$

Because our main concern is the onset of flutter instability, particular attention is paid in this paper to the behaviour of the frequency-response component of the lift force. It should be remarked that inequality (3) is valid regardless of whether the lift force in vortex excitation is locked in (see the discussions on vortex excitation in §4).

2.5. *Combined blockage and end effects*

In an experiment using a sectional model with end plates, combined blockage and end effects should be considered (Nakamura & Nakashima 1986). Generally, the two effects have opposite signs: namely, the former decreases the base pressure of a bluff body whereas the latter increases it. In the present experiment the blockage ratio was as large as 5.0 % and the size of the end plates used was relatively small. However, none of the results presented have been corrected for these two effects since there

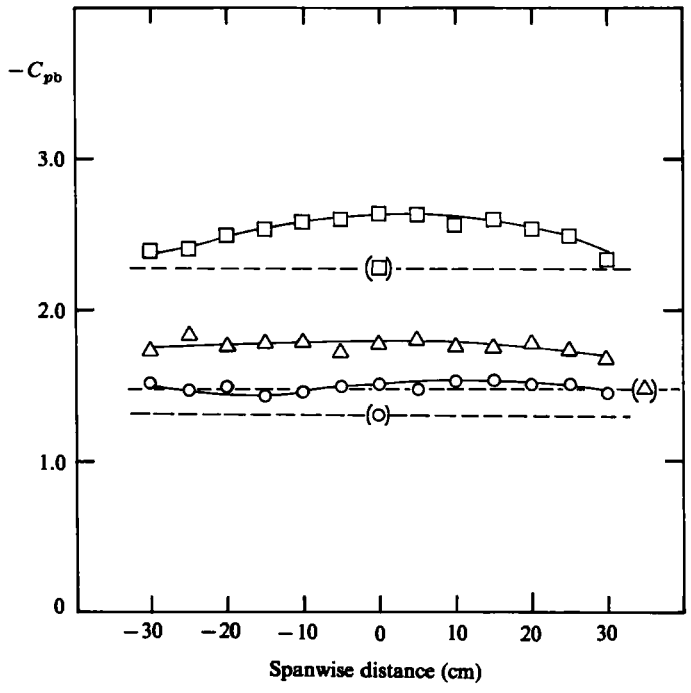

FIGURE 2. Spanwise distributions of the mean base-pressure coefficient of fixed rectangular cylinders. ○, $d/h = 0.2$; △, 0.4; □, 0.6; ----, corrected value (Nakamura & Ohya 1984).

is no method of correction available for fluctuating force measurements made with an oscillating bluff body.

3. Experimental results

3.1. *Mean base pressure of forced-oscillating cylinders*

Figure 2 shows the spanwise distributions of the mean base-pressure coefficient of fixed rectangular cylinders with three different values of the side ratio. It also includes the corresponding corrected values of Nakamura & Ohya (1984) for a comparison. It is seen that the base pressure of cylinders with $d/h = 0.2$ and 0.4 is reasonably uniform along the span while it is non-uniform for the cylinder with $d/h = 0.6$, which is close to the critical section with $d/h = 0.67$ at which the base pressure shows a sharp minimum (Nakaguchi, Hashimoto & Muto 1968; Bearman & Trueman 1972).

Figure 3(*a–c*) shows the variations of the mean base-pressure coefficients of rectangular cylinders oscillating at amplitudes of $0.05h$ and $0.1h$ with the reduced wind speed. It is interesting that the mean base pressure is decreased considerably near the vortex-resonant speed $\overline{U}_{cr}$ for cylinders with $d/h = 0.2$ and 0.4 while little departure from the steady-state value is seen for the cylinder with $d/h = 0.6$. The mean base pressure at reduced wind speeds much lower than $\overline{U}_{cr}$ is also smaller than the steady-state value for the former two, while it is larger for the cylinder with $d/h = 0.6$.

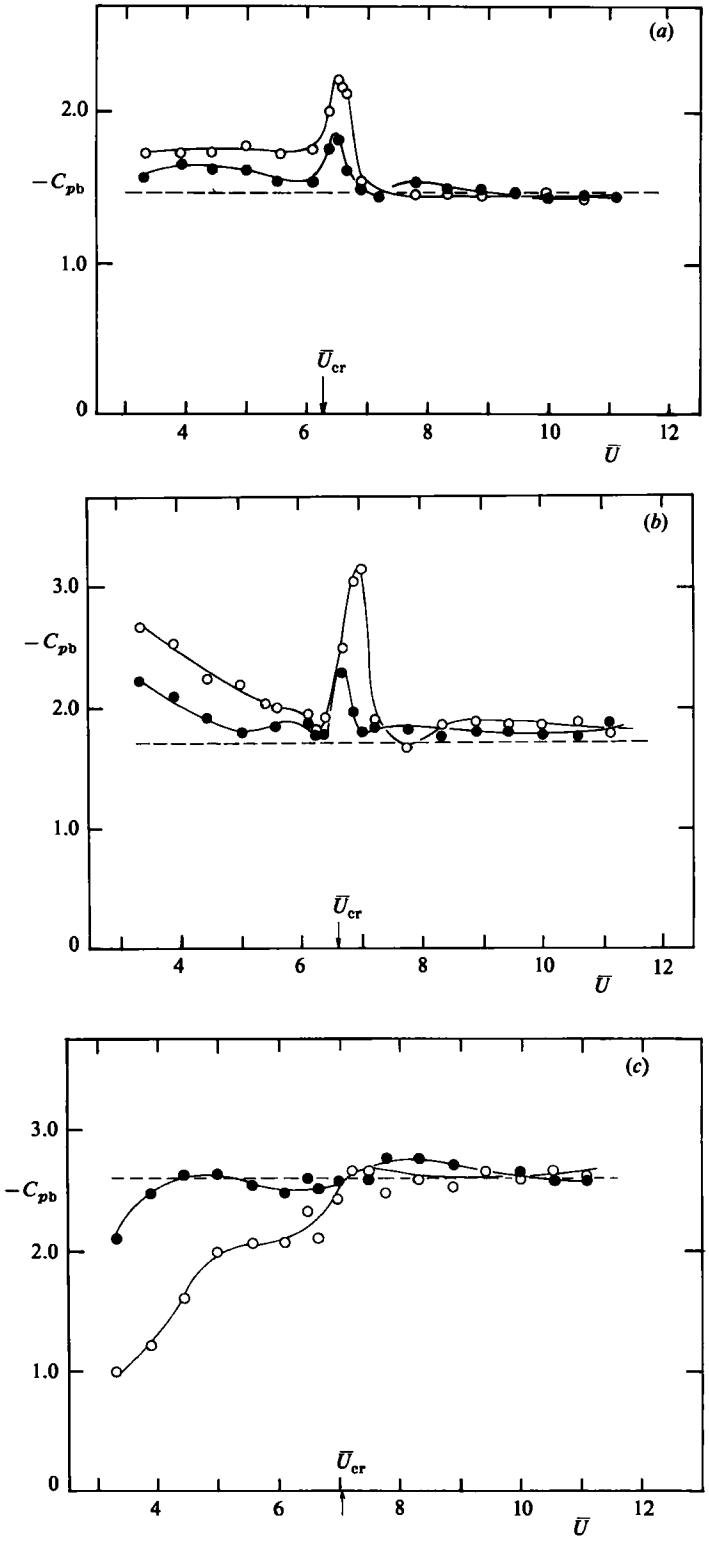

FIGURE 3. For caption see facing page.

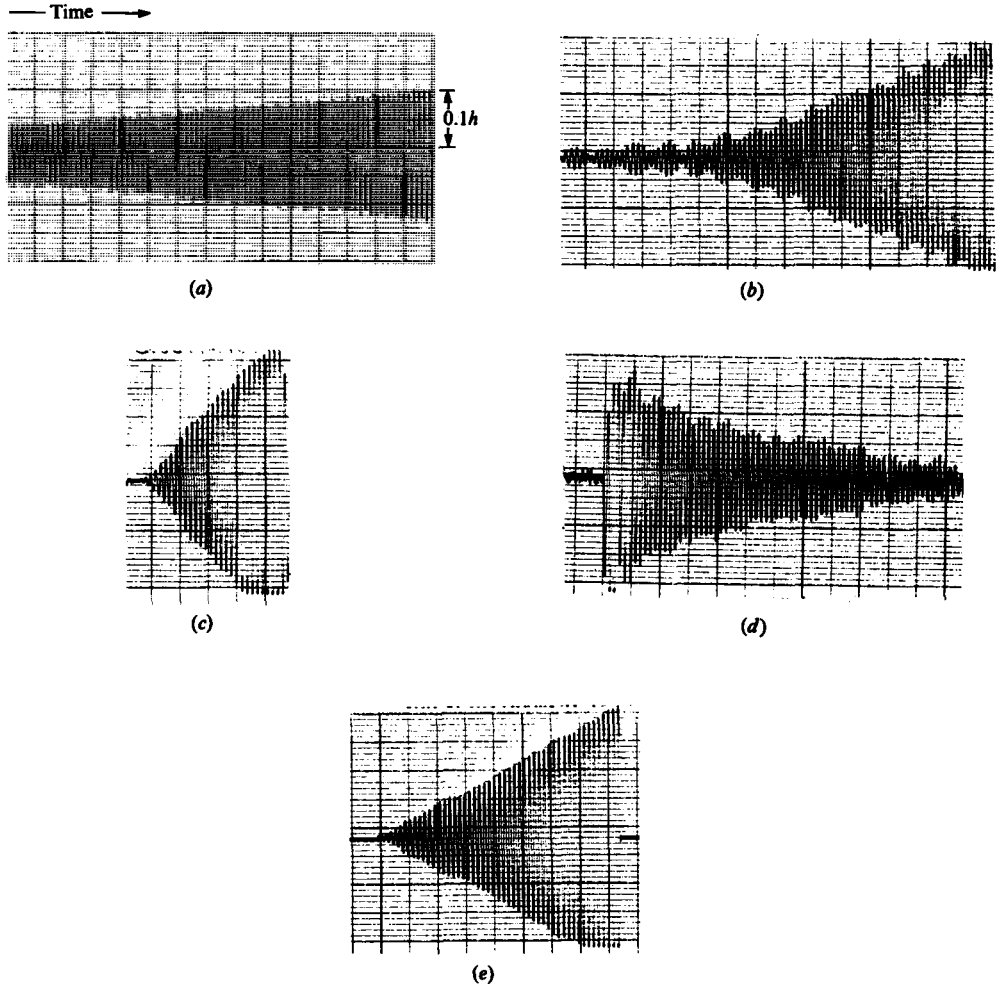

FIGURE 4. Traces of the cylinder-displacement signal in the free-oscillation experiment. (*a*) $d/h = 0.4$, $\overline{U} = 4.17$; (*b*) 0.4, 5.36; (*c*) 0.4, 6.30; (*d*) 0.4, 11.9; (*e*) 0.2, 6.14.

3.2. *The rate of growth of oscillation of freely oscillating cylinders*

Figure 4 shows samples of the displacement signal during the growth of oscillation of cylinders with $d/h = 0.2$ and 0.4 at various wind speeds. The dominant frequency of oscillation in wind remained the same as that in still air because of the large mass ratio. The results for the logarithmic rate of growth β_a at an amplitude of $0.1h$ are shown in figure 5(*a*–*c*) for the three cylinders with and without a splitter plate. The rate of growth β_a is defined by the relation $\beta_a = \beta + \delta_s$, where β is the logarithmic rate of growth in wind, and hence it represents the aerodynamic contribution to the logarithmic rate of growth in wind. An estimate of β_a using the forced-oscillation data is also given in each of the figures for a later discussion.

FIGURE 3. Mean base-pressure coefficients versus reduced wind speed for forced-oscillating rectangular cylinders. (*a*) $d/h = 0.2$, (*b*) 0.4, (*c*) 0.6: ●, oscillation amplitude $y_0/h = 0.05$; ○, 0.1; – – –, value for fixed cylinder.

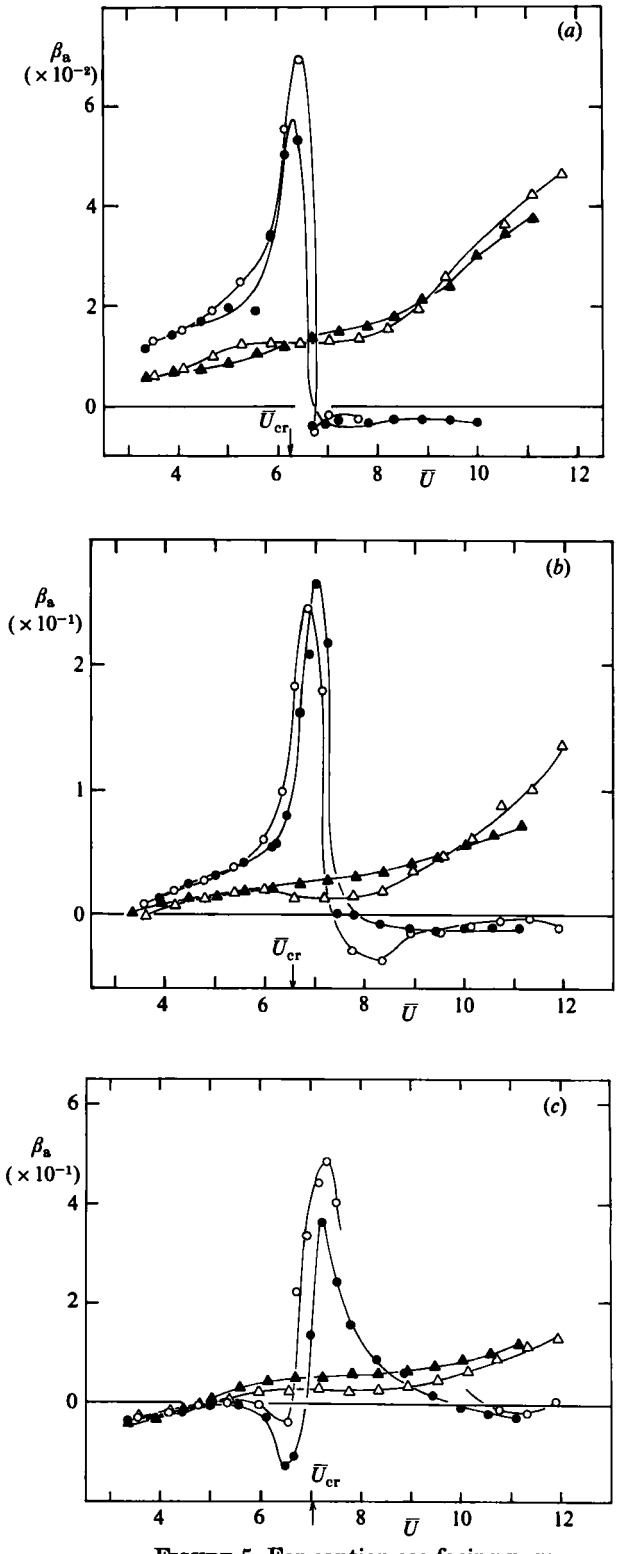

FIGURE 5. For caption see facing page.

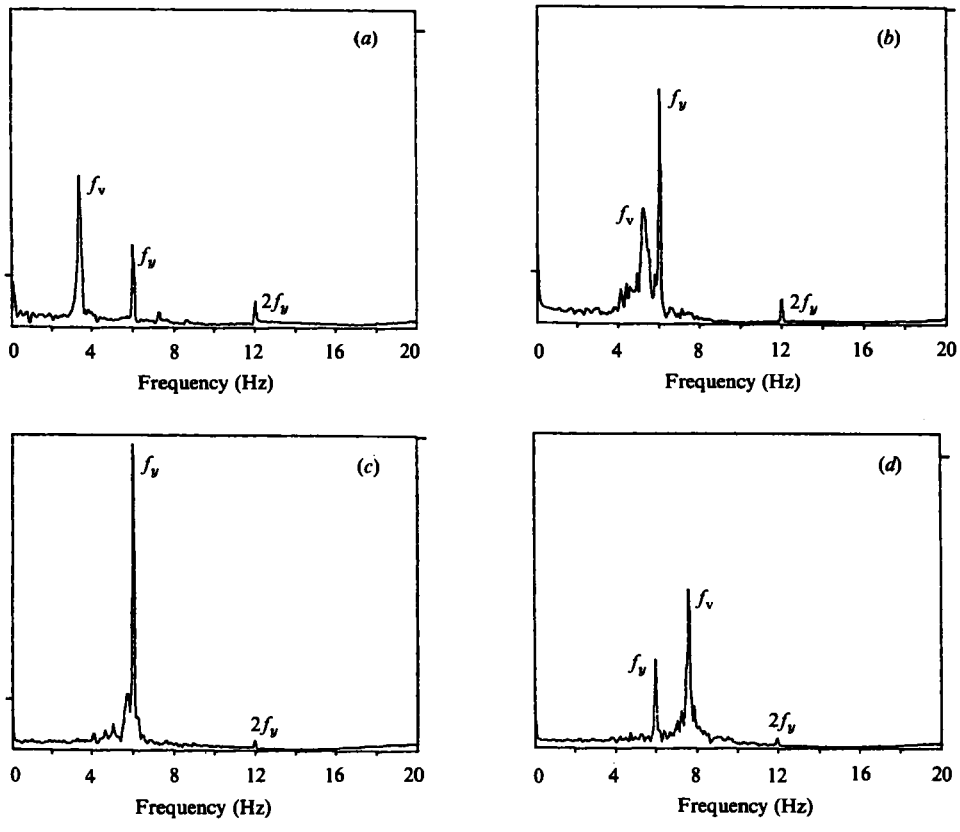

FIGURE 6. Samples of the power spectrum of fluctuating lift force on a cylinder with $d/h = 0.4$ oscillating at $y_0/h = 0.1$. (*a*) $\overline{U} = 3.9$, $\overline{U}/\overline{U}_{cr} = 0.59$; (*b*) 6.1, 0.93; (*c*) 7.0, 1.06; (*d*) 8.3, 1.26.

It is seen from figure 5 that all three cylinders are vortex excited and excitation becomes more violent with increasing d/h. One of the features of vortex excitation is that the oscillation is not always built up exponentially, i.e. when expressed by $e^{\lambda t} \sin 2\pi f_y t$, λ is not constant but amplitude dependent. Another feature to mention is beat modulation. These are seen in the signal traces in figure 4. Beat modulation was weakest for the cylinder with $d/h = 0.2$ while it was most severe for the cylinder with $d/h = 0.6$, which made measurement of the rate of growth sometimes difficult.

It is seen from figure 5(*a*, *b*) that a weak instability was built up at low wind speeds well below $\overline{U}_{cr}$, say, around $\overline{U} = 4.0$, for cylinders with $d/h = 0.2$ and 0.4. An example of the signal trace for this low-speed flutter is given in figure 4(*a*). At high wind speeds no galloping was observed on any of the three cylinders. This is in agreement with a previous measurement (Nakamura & Tomonari 1977) where it was shown that high-speed galloping can occur only for sections longer than the critical with $d/h = 0.67$.

Low-speed flutter is also seen to occur for cylinders with a splitter plate. No vortex

FIGURE 5. The logarithmic rate of growth of oscillation versus reduced wind speed for rectangular cylinders with and without a splitter plate. (*a*) $d/h = 0.2$, (*b*) 0.4, (*c*) 0.6: ○, ●, cylinder without a splitter plate; △, ▲, cylinder with a splitter plate: open symbols, direct measurements in free-oscillation experiment; black symbols, equation (4) using forced-oscillation data.

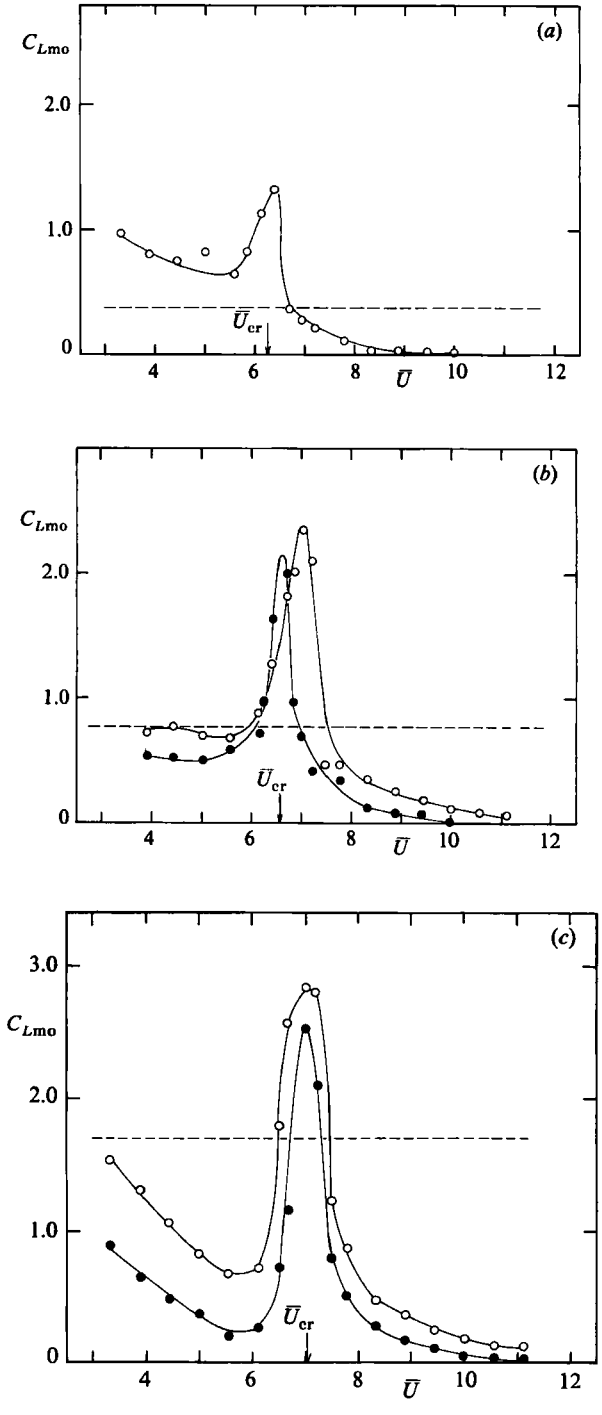

FIGURE 7. Magnitude of the frequency-response component of fluctuating lift-force coefficient of a rectangular cylinder. (*a*) $d/h = 0.2$, (*b*) 0.4, (*c*) 0.6: ●, $y_0/h = 0.05$, ○, 0.1; ——, value for a fixed cylinder with f_v.

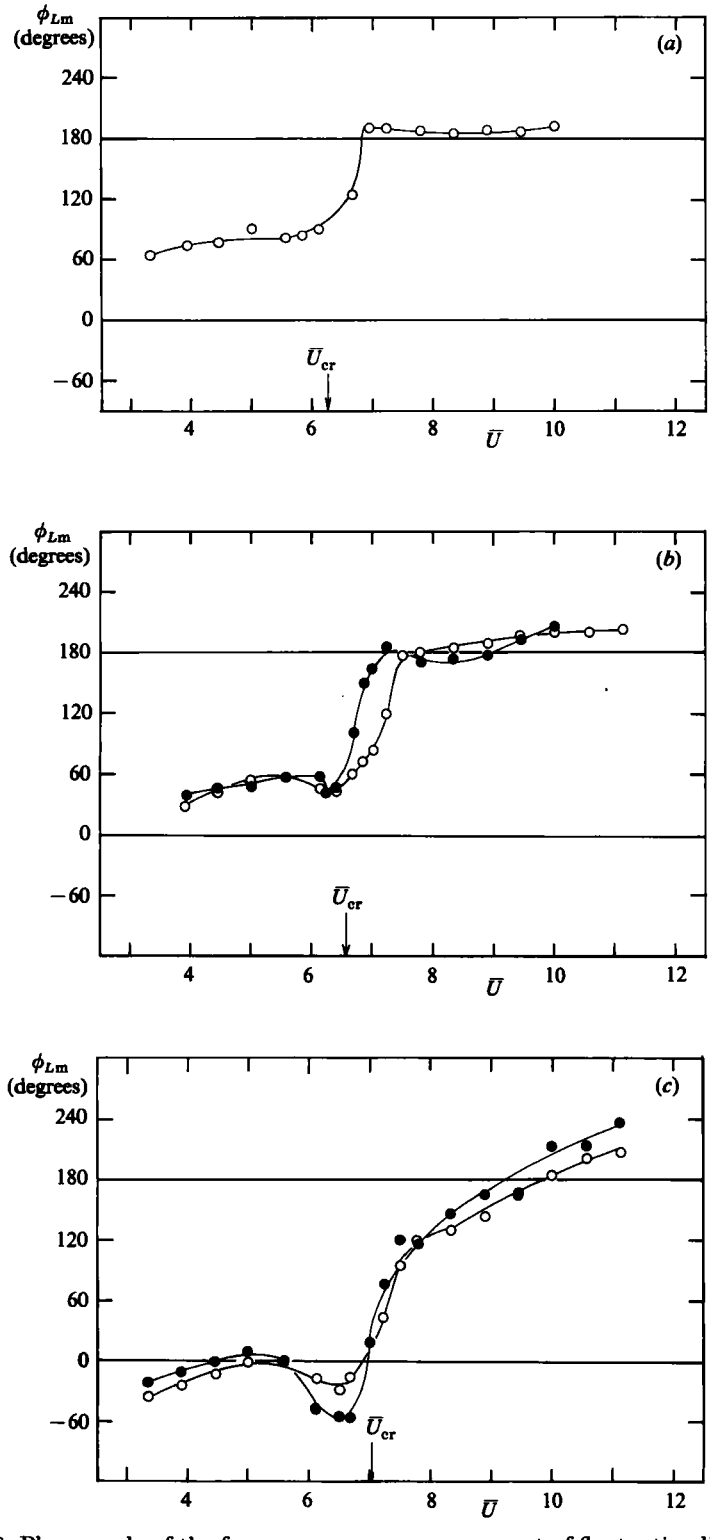

FIGURE 8. Phase angle of the frequency-response component of fluctuating lift-force coefficient of a rectangular cylinder. (*a*) $d/h = 0.2$, (*b*) 0.4, (*c*) 0.6: ●, $y_0/h = 0.05$; ○, 0.1.

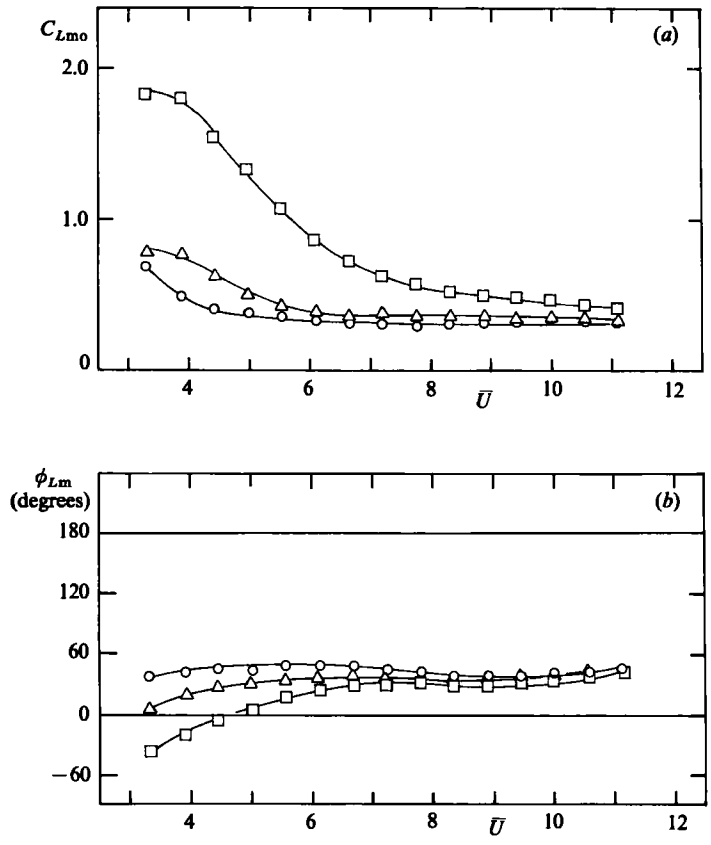

FIGURE 9. Frequency-response component of fluctuating lift-force coefficient of a rectangular cylinder with a splitter plate. (*a*) magnitude, (*b*) phase angle: ○, $d/h = 0.2$; △, 0.4; □, 0.6.

excitation was observed on any of the cylinders with a splitter plate. Instead, a very regular instability was built up and continued up to high wind speeds, in agreement with Nakamura & Tomonari (1977).

3.3. *Fluctuating lift force on forced-oscillating cylinders*

Figure 6 shows samples of the power spectrum of the fluctuating lift force on the cylinder with $d/h = 0.4$. At wind speeds well away from the vortex-resonant speed $\bar{U}_{cr}$ (figure 6*a* and *d*), the Strouhal component is dominant over the frequency-response component with $f_y = 6.0$ Hz. At wind speeds close to $\bar{U}_{cr}$ (figure 6*c*) the Strouhal frequency is locked in to that of the imposed body frequency at a sufficiently large amplitude.

The variations of the magnitude of the frequency-response component of the lift force for amplitudes of the imposed body oscillation of $0.05h$ (except for $d/h = 0.2$) and $0.1h$ with the reduced wind speed are shown in figure 7(*a–c*), while those of the phase angle are shown in figure 8(*a–c*). The values of the lift force on fixed cylinders are also included in figure 7(*a–c*).

It is seen that while vortex excitation is characterized by several nonlinear phenomena such as lock-in, the lift force still retains the resonance characteristics of a linear oscillator; namely, it exhibits a sharp peak in magnitude and a rapid

change in phase angle (amounting to about 180° for the cylinder with $d/h = 0.6$) through vortex resonance. Lift amplification at vortex resonance is most significant for the cylinder with $d/h = 0.2$. Figure 8 (a, b) indicates the onset of low-speed flutter for cylinders with $d/h = 0.2$ and 0.4. The results of the lift-force measurement for cylinders with a splitter plate at an amplitude of the imposed oscillation of $0.1h$ are shown in figure 9 (a, b).

4. Discussion of the experimental results

4.1. *Three distinct flow ranges*

The response of the flow past a bluff body to the imposed body oscillation consists of two main parts. One is the flow response linked directly to the acceleration of the body, and the other is the flow response to the continual variation of the angle of incidence of the body. The flow response to the body acceleration is dominant at low wind speeds, but it is less significant relative to the onset of flutter. As is shown in inequality (3), the onset of flutter is directly associated with the out-of-phase component of the lift force, however small in magnitude.

The variation of the angle of incidence produces undulation of the wake, the wavelength of which is progressively shortened with decreasing wind speed. Wake undulation can manifest itself as motion-dependent vortices when the wind speed is low enough and the amplitude of the imposed oscillation is sufficiently large. However, it should be noted that the influence of the imposed oscillation is present as wake undulation at any wind speed whether or not it manifests itself as motion-dependent vortices.

When the frequency of the imposed oscillation approaches that of natural vortex shedding, a strong resonant interaction can occur between wake undulation and natural vortex shedding. As we have seen, the dynamic flow response due to resonance is restricted to a narrow range of the wind speed. On this basis three distinct flow ranges of interest can be identified: the low-speed flow range where $f_y \gg f_v$, the range of vortex resonance where $f_y \approx f_v$, and the high-speed flow range where $f_y \ll f_v$. The distortion of the time-mean flow due to the imposed body oscillation should also be considered to gain a better understanding of the dynamic flow response. Since vortex excitation is a strongly nonlinear phenomenon, resonant interaction can vitally influence the time-mean flow.

4.2. *Critical side ratio of forced-oscillating rectangular cylinders*

In his study of the flow past oscillating rectangular cylinders Mizota (1984) measured the mean base pressure of a rectangular cylinder oscillating externally at vortex resonance over a wide range of d/h. The results of his measurement are reproduced in figure 10 together with the present results. It can be seen that the base pressure of an oscillating rectangular cylinder shows a sharp minimum at $d/h = 0.4$: namely, the side ratio $d/h = 0.4$ is critical for rectangular cylinders oscillating at resonance just as the side ratio $d/h = 0.67$ is for fixed rectangular cylinders. Oscillating rectangular cylinders with d/h below the critical value may be termed as short in this sense and those beyond the critical may be termed as long. It is also interesting that a rectangular cylinder with $d/h = 0.6$ has no peak of $-C_{pb}$ at resonance. According to Bearman & Obasaju (1982), a weak peak near resonance reappears for a square cylinder.

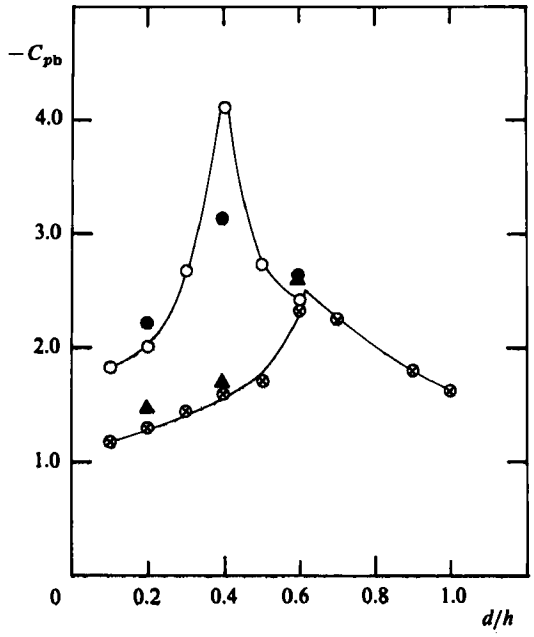

FIGURE 10. Mean base-pressure coefficient versus side ratio for fixed and oscillating rectangular cylinders. ▲, fixed; ●, oscillating at $y_0/h = 0.1$: ○, ⊗, Mizota (1984).

4.3. *Comparison between the results of free- and forced-oscillation experiments*

It has been assumed in the past (see, for example, Nakamura 1978) that the frequency and the rate of growth of slightly growing or decaying oscillation of a flexibly mounted body in the flow can be estimated with reasonable accuracy by using the frequency-response components of the aerodynamic forces and moment, and vice versa. This assumption is also examined in the present investigation. The rate of growth of oscillation is given in terms of the out-of-phase component of the lift force as

$$\beta_a = \left(\frac{\overline{U}^2}{8\pi\mu}\right)\left(\frac{d}{y_0}\right) C_{Lmo} \sin\phi_{Lm}. \tag{4}$$

This is compared with the directly measured one in figure 5(*a–c*). It is seen that agreement is good over the wind-speed range tested for the three rectangular cylinders with and without a splitter plate. In particular, agreement is fairly good even for vortex excitation where the rate of growth of oscillation is amplitude dependent.

4.4. *Low-speed flutter*

The mechanism of onset of low-speed flutter that occurred for cylinders with $d/h = 0.2$ and 0.4 is unknown and merits further investigation. However, it is interesting that the instability was also observed on cylinders with a splitter plate. A reasonable interpretation of this fact is that the flow downstream of a bluff body cannot adjust the upstream flow effectively when oscillation is fast enough. This is one of the most remarkable features of the oscillatory flow past a bluff body, and has been mentioned earlier for bluff cylinders with elongated cross-sections (Nakamura & Nakashima 1986).

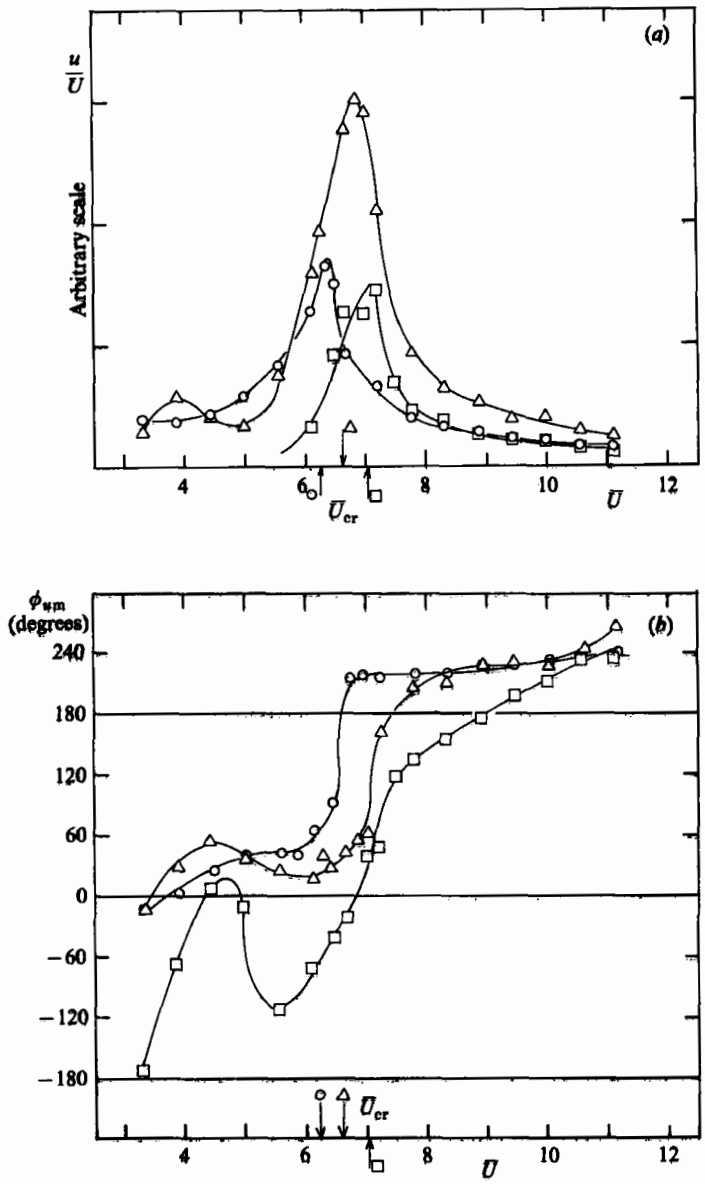

FIGURE 11. Frequency-response component of fluctuating velocity in the wake of an oscillating rectangular cylinder. (*a*) magnitude, (*b*) phase angle: ○, $d/h = 0.2$; △, 0.4; □, 0.6.

4.5. *Vortex resonance*

As has already been mentioned, the frequency-response component of the lift force in the range of vortex resonance, although showing a number of nonlinear characteristics, still retains the important resonance characteristics of a linear oscillator; namely, a sharp peak in magnitude and a rapid change in phase angle through vortex resonance.

The resonance characteristics can be found not only in the lift force but also in various other flow parameters. A rapid change in the phase angle of the surface

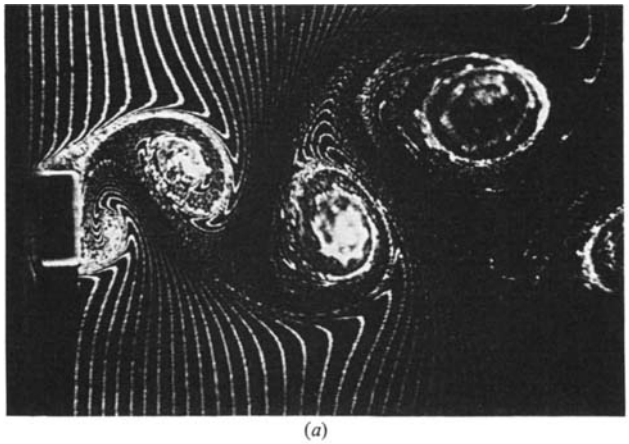

(*a*)

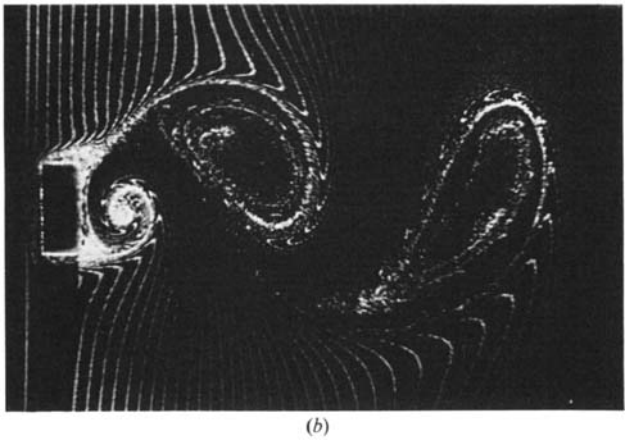

(*b*)

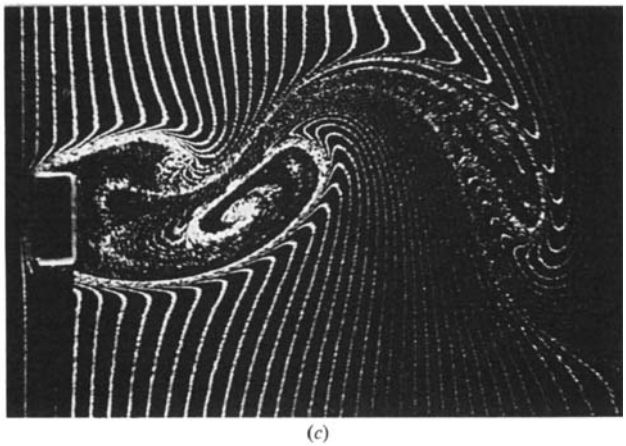

(*c*)

FIGURE 12. Flow past a rectangular cylinder with $d/h = 0.4$ oscillating at $y_0/h = 0.25$ at the Reynolds number of 177. (*a*) $\overline{U} = 6.25$ ($= \overline{U}_{cr}$), (*b*) 6.58, (*c*) 6.94. The photographs correspond to the instant when the cylinder is at an extreme downward position.

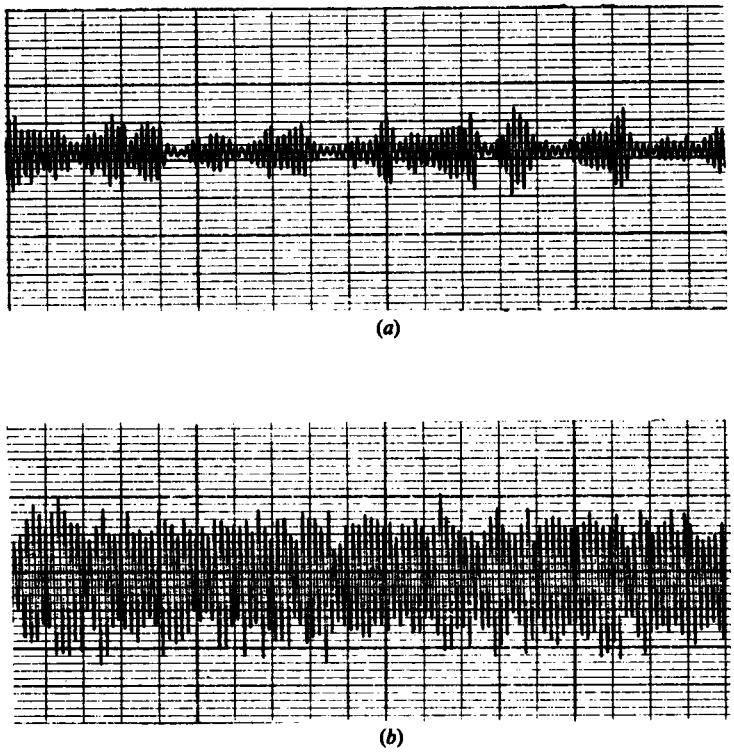

FIGURE 13. Traces of fluctuating lift-force signal of a rectangular cylinder with $d/h = 0.2$. (*a*) fixed cylinder, (*b*) cylinder oscillating at $\overline{U}_{cr}$ with $y_0/h = 0.1$.

pressure of an oscillating circular cylinder has been demonstrated by Feng (1968) and Bearman & Currie (1979). Figure 11 (*a*, *b*) shows the results for the velocity fluctuation in the wake of the three rectangular cylinders oscillating at an amplitude of $0.1h$. They suggest a strong resonant interaction between wake undulation and natural vortex shedding.

In particular, the phase angle of the fluctuating velocity changes by roughly 180° through vortex resonance for all the three rectangular cylinders. The photographs in figure 12 (*a–c*), taken in a water-tank experiment using a hydrogen-bubble method, show the flow past a rectangular cylinder with $d/h = 0.4$, where $h = 1$ cm, which is oscillating at a flow speed of 2.5 cm s^{-1} at an amplitude of $0.25h$ with frequencies of 0.4 Hz ($\overline{U} = \overline{U}_{cr} = 6.25$), 0.38 Hz ($\overline{U} = 6.58$) and 0.36 Hz ($\overline{U} = 6.94$). The Reynolds number was equal to 177. Vortex shedding was completely locked-in to the imposed body oscillation over the range of vortex resonance because of a large oscillation amplitude. The photographs, taken with an exposure time of $\frac{1}{60}$ s, correspond to the instant when the cylinder was at an extreme downward position. It is seen that the phase angle of vortex shedding relative to the cylinder motion undergoes a rapid change through vortex resonance. Similar results of flow visualization were reported by Zdravkovich (1982) on an oscillating circular cylinder.

One of the nonlinear effects on vortex excitation is found in the lift amplification at resonance. The rate of amplification is largest for the cylinder with $d/h = 0.2$ where the magnitude of the lift force at an amplitude of $0.1h$ of the imposed body oscillation is approximately 3.5 times that of a fixed cylinder (figure 7*a*). Two traces of the

lift-force signal of the cylinder with $d/h = 0.2$ are shown in figure 13(a, b); one for the fixed cylinder and one for the cylinder oscillating at the vortex-resonant frequency. The signal in figure 13(a) is characterized by large random modulation while that in figure 13(b) indicates much reduction in this due to the imposed body oscillation. The maximum of the lift amplitude in figure 13(b) is approximately twice that in figure 13(a). This value of the lift amplification is considerably smaller than the value of 3.5 just mentioned. Obviously, the difference between the two is attributable to the reduction in amplitude modulation due to the imposed body oscillation.

4.6. *$t \sin t$-type divergence*

Beat modulation can be observed in vortex excitation where the natural vortex-shedding frequency f_v is close to but different from the body frequency f_y. It is interesting to see what happens at the vortex-resonant speed where f_v is exactly equal to f_y. We have found that the oscillation exhibits a $t \sin t$-type divergence up to a relatively large amplitude beyond $0.1h$ (see figure 4c and e, for example). If the body oscillation is given by $y(t) = ct \sin 2\pi f_y t$, where c is a constant, the lift force per unit span acting on the body is obtained by using the equation of motion, which neglects the system damping for simplicity, as

$$\begin{aligned} L(t) &= m\ddot{y} + m(2\pi f_y)^2 y \\ &= 4\pi m c f_y \cos 2\pi f_y t. \end{aligned} \tag{5}$$

The lift force is thus a sinusoidal oscillation with a phase angle of 90°.

4.7. *The onset of vortex excitation*

The foregoing analysis suggests that the phase angle of the lift force in the range of vortex resonance depends on the level in the low-speed flow range and the subsequent rapid change due to resonance. Vortex excitation can occur when the phase angle falls in the unstable region which is given by inequality (3).

For the cylinder with $d/h = 0.2$, vortex excitation follows low-speed flutter continuously with increasing wind speed (figure 8a). In this case vortex excitation is extended on either side of the vortex-resonant speed $\overline{U}_{cr}$. As d/h is increased the phase angle of the lift force in the low-speed flow range is progressively decreased ($d/h = 0.4$) and eventually falls in the stable region ($d/h = 0.6$); the phase angle of the cylinder with $d/h = 0.6$ is not constant at low speeds but shows an overshoot before entering into the range of vortex resonance. As a result, the oscillation of the cylinder with $d/h = 0.6$ is stable in the lower half of the vortex-resonance range despite a large phase-angle change. It is only in the upper half of the vortex-resonance range that excitation can occur. This trend is further amplified with increasing d/h. Bearman & Obasaju (1982) noted that vortex excitation of a square cylinder was limited to a narrow range at the upper end of vortex resonance (or at the upper end of lock-in in their terminology).

4.8. *Vortex excitation as coupled flutter*

It is now clear that vortex excitation is a flow-induced, self-excited oscillation of a bluff body, and hence it is categorized under the heading of aeroelastic flutter. Vortex excitation as flutter is characterized as follows. The system that we consider consists of two oscillatory subsystems; one is the body subsystem which has a natural frequency of f_y, and the other is the fluid subsystem which has a natural frequency of f_v. The two subsystems are strongly coupled in such a way that the body subsystem

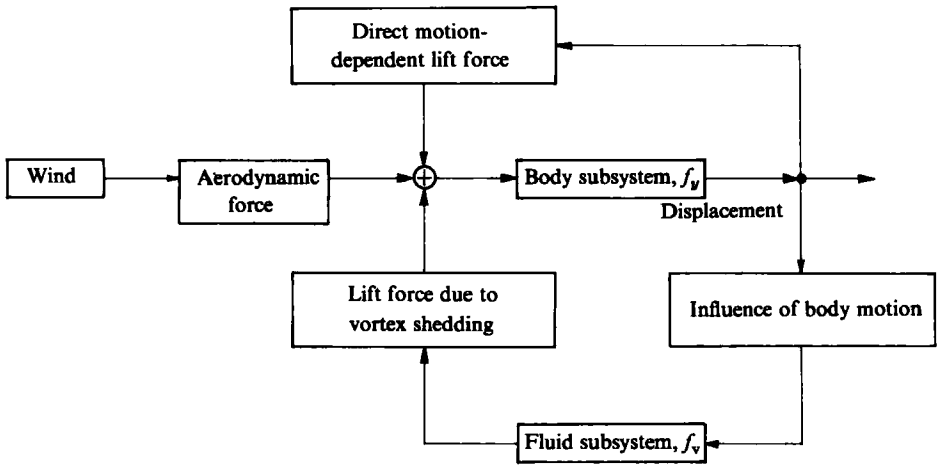

FIGURE 14. Block diagram showing the response of a bluff body in the presence of vortex shedding.

is driven by the fluctuating lift force due to vortex shedding in addition to the direct motion-dependent lift force, while the fluid subsystem is in turn influenced significantly by the body motion. Thus, vortex excitation can be identified as coupled flutter occurring in a body–fluid system. Figure 14 is a block diagram illustrating the response of a bluff body in the presence of vortex shedding. The concept of vortex excitation as coupled flutter was proposed earlier by Nakamura & Mizota (1975) and Ito & Nakamura (1982).

The basic instability mechanism of coupled flutter is that the cross-coupling force can do positive work in the presence of a phase difference between different degrees of freedom. In the classical example of bending–torsion flutter of an aircraft wing, the lift force due to torsion can amplify the bending motion of the wing if there is a favourable phase difference between bending and torsion. The same instability mechanism can be applied to other dynamical systems with many degrees of freedom. According to Stuart (1971), the boundary-layer instability can occur when the Reynolds stress becomes positive in the presence of a phase difference between the u- and v-velocity components.

The essential feature of vortex excitation as coupled flutter is that the natural frequency of the fluid subsystem f_v is proportional to the wind speed. The imposed body motion can set the fluid subsystem into resonance when the vortex-resonant speed is approached. The phase angle of the lift force due to vortex shedding relative to the body motion undergoes a rapid change through vortex resonance. This in turn produces a large out-of-phase component of the lift force so that the body motion is amplified.

4.9. *High-speed flow range*

No drastic changes have been observed in the lift-force characteristics in the high-speed flow range where the natural vortex-shedding frequency f_v is much higher than the body frequency f_y. With increasing wind speed, the flow appears to gradually approach that past a fixed cylinder, although several other types of flutter such as galloping and torsional flutter characterize this particular flow range. The mechanism of onset of flutter observed on cylinders with a splitter plate is unknown and merits further investigation.

4.10. *Some remarks on the concept of lock-in*

In the present paper the term vortex resonance has been chosen in preference to lock-in to describe vortex excitation. As we have seen, the onset of vortex excitation is limited to a certain range of vortex resonance. Vortex resonance is a feature of a linear oscillator while lock-in is a typical nonlinear phenomenon. Therefore, lock-in is neither equivalent to vortex resonance nor to vortex excitation.

5. Conclusions

Vortex excitation of a bluff body is an aeroelastic flutter occurring in a fluid–body system where the two subsystems strongly interact with each other; in short, it is classified as coupled flutter. The most essential feature of vortex excitation as coupled flutter is that the fluid subsystem can be set into resonance by the body motion. A rapid phase-angle change of the lift force through vortex resonance produces a large out-of-phase force component which excites the motion of the body subsystem.

Vortex excitation of a rectangular cylinder is strongly dependent on the side ratio. It appears that the critical change in the mean base pressure of an oscillating rectangular cylinder with increasing side ratio is closely correlated with the vortex-excitation characteristics. For short rectangular cylinders, vortex excitation follows low-speed flutter and is extended on either side of the vortex-resonant speed. For long rectangular cylinders, vortex excitation is limited to the upper half of the vortex-resonance range since low-speed oscillation is stable. Also, the lift amplification in vortex excitation of short rectangular cylinders is much larger than that of long rectangular cylinders.

In the present paper attention has been confined to vortex excitation caused by the Kármán vortex trail. For rectangular cylinders with d/h greater than about 3.0 and other elongated bluff cylinders, vortex excitation is not caused by the Kármán vortex trail but by the impinging-shear-layer instability where a single separated shear layer becomes unstable in the presence of a sharp trailing edge (Nakamura & Nakashima 1986). For a rectangular cylinder with $d/h = 2.0$, close to the transition point, it has been shown (Nakamura & Mizota 1975) that vortex excitation is very much distorted and the lift-force characteristics are strongly amplitude dependent.

We thank Dr T. Mizota, now of the Fukuoka Institute of Technology, and Messrs N. Fukamachi, K. Watanabe and K. Sugitani for assistance in conducting the experiments.

REFERENCES

Bearman, P. W. 1984 *Ann. Rev. Fluid Mech.* **16**, 195–222.

Bearman, P. W. & Currie, I. G. 1979 *J. Fluid Mech.* **91**, 661–677.

Bearman, P. W. & Obasaju, E. D. 1982 *J. Fluid Mech.* **119**, 297–321.

Bearman, P. W. & Trueman, D. M. 1972 *Aero Q.* **23**, 229–237.

Feng, C. C. 1968 MASc. thesis, Faculty of Engineering, University of British Columbia, Canada.

Ito, M. & Nakamura, Y. 1982 *IABSE Surveys* S-20/82. International Association for Bridge and Structural Engineering.

Mizota, T. 1984 Doctoral thesis, Faculty of Engineering, Kyushu University, Japan (in Japanese).

Nakaguchi, H., Hashimoto, K. & Muto, S. 1968 *J. Japan. Soc. Aero. Space Sci.* **16**, 1–5 (in Japanese).

Nakamura, Y. 1978 *J. Sound Vib.* **57**, 471–482.

NAKAMURA, Y. 1979 *J. Sound Vib.* **67**, 163–177.

NAKAMURA, Y. & MIZOTA, T. 1975 *J. Eng. Mech. Div. ASCE* **101**, (EM6) 855–871.

NAKAMURA, Y. & NAKASHIMA, M. 1986 *J. Fluid Mech.* **163**, 149–169.

NAKAMURA, Y. & OHYA, Y. 1984 *J. Fluid Mech.* **149**, 255–273.

NAKAMURA, Y. & TOMONARI, Y. 1977 *J. Sound Vib.* **52**, 233–241.

OTSUKI, Y., WASHIZU, K., TOMIZAWA, H. & OHYA, A. 1974 *J. Sound Vib.* **34**, 233–248.

SARPKAYA, T. 1979 *Trans. ASME* E: *J. Appl. Mech.* **46**, 241–258.

STUART, J. T. 1971 *Mathematical Problems in Geophysical Sciences.* Lectures in Applied Mathematics, vol. 13, pp. 139–155. American Math. Soc.

WASHIZU, K., OHYA, A., OTSUKI, Y. & FUJII, K. 1978 *J. Sound Vib.* **59**, 195–210.

WILKINSON, R. H. 1974 Ph.D. thesis, Faculty of Engineering, University of Bristol, England.

ZDRAVKOVICH, M. M. 1982 *Trans. ASME* I: *J. Fluids Engng* **104**, 513–517.